

Modeling The Effects of Leakage Inductance On Flyback Converters (Part 2): The Average Model

by Christophe Basso, ON Semiconductor, Toulouse, France

In the [first part](#) of this article, we have described the switching effects produced by the leakage inductance: a reduced effective duty ratio bringing an extension of the secondary-diode conduction time and a delay in the appearance of the secondary-side current after the main switch has been turned off. As a result, the output voltage is lower than what the original formula (equation 21 in part 1) predicts and power dissipation increases in the RCD clamping network. Given the impact of the leakage term on operating waveforms, it is interesting to investigate its influence on the small-signal response of the flyback converter.

However, before we perform small-signal analysis, we need a good average (or large-signal) model. We will develop this model here by applying Vorpérian's PWM switch model to the CCM flyback converter with adjustments (based on results from part 1) to account for the effects of leakage inductance. But first, we will revisit the cycle-by-cycle model to demonstrate the effects of leakage inductance on the load-step response of the converter.

The Response To A Load Step

The cycle-by-cycle model introduced in part 1 appears in Fig. 1 and now includes a variable load. In this simulation, the load will vary from 8 Ω to 6 Ω in a 10- μ s span while the output is recorded. The converter runs in an open-loop configuration and we will increase the leakage inductance from 1 μ H to 50 μ H while the rest of operating parameters are kept constant (40% duty ratio).

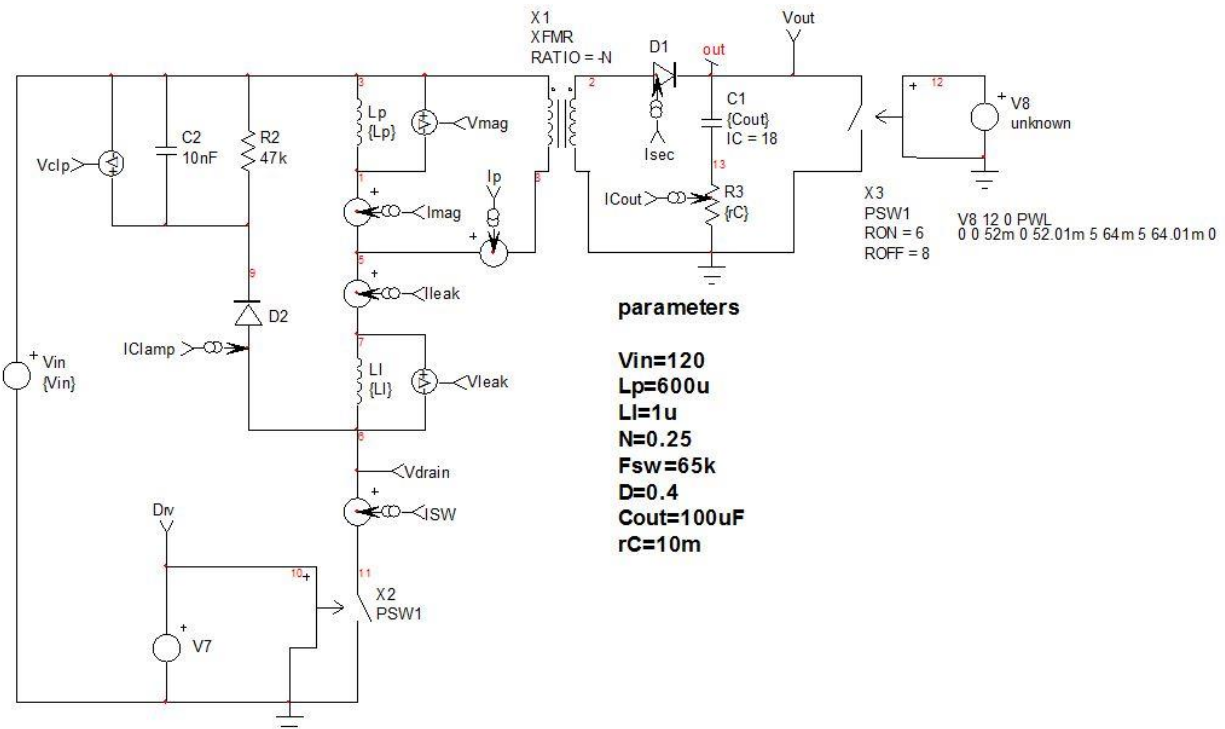


Fig. 1. This simplified flyback converter, which is configured for open-loop operation, will let us explore the effects of the leakage inductance.

In Fig. 2, we have gathered the output voltage waveforms obtained for various values of leakage inductance. The vertical scale is 620 mV per division and common to each waveform but the offset is adjusted to allow all the curves to be displayed in the same graph.

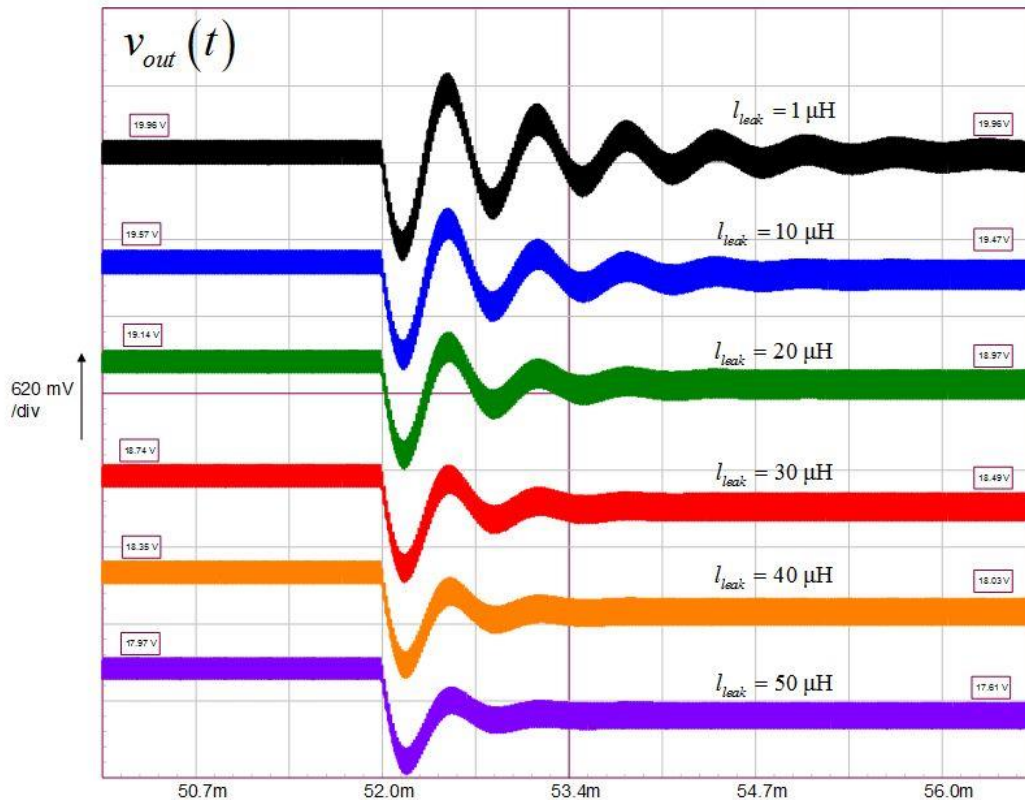


Fig. 2. Varying the leakage inductance affects several parameters of the open-loop flyback converter.

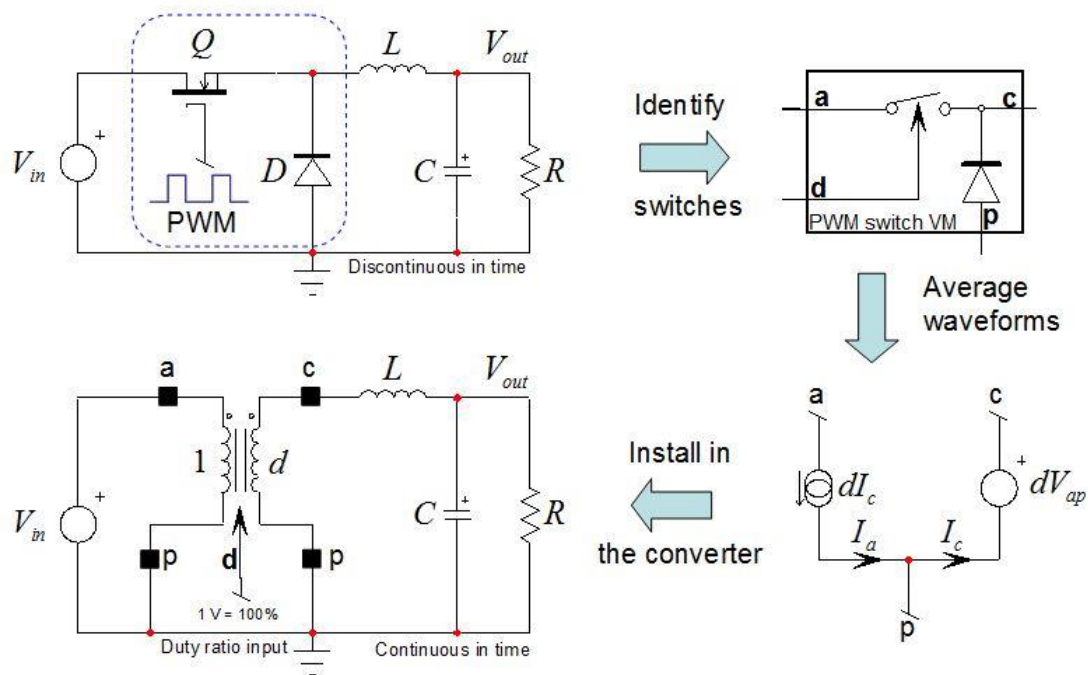
The first thing to observe in these simulations of the converter's load-step response is the ringing. With almost no leakage inductance (1 μ H), the response rings and damping is light. However, the step in the load current does not affect the output voltage. As the leakage inductance grows, ringing starts to dampen and oscillations cease quickly for $l_{leak} = 50 \mu$ H. However, the more leakage inductance you have, the lower the output voltage (it drops from almost 20 V to 17.6 V) and the deeper the static voltage drop: almost 0 V with no leakage and up to 400 mV with the biggest leakage inductance.

From this quick simulation, we can observe that the leakage inductance damps the transient response, affects the steady-state output voltage (as predicted in part 1) but also degrades the output impedance. To explore the impact of the leakage inductance on the frequency response, we need a large-signal model later linearized to give a small-signal representation of our converter. From this small-signal model, we should be able to analytically express the control-to-output transfer function of the flyback converter in a way that accounts for the effect of leakage inductance.

A Large-Signal Model

The PWM switch lends itself very well to modeling a flyback converter. Introduced by Vatché Vorpérian in the 90s^[1], the simplest version to model the large-signal response of a two-switch voltage-mode dc-dc converter operated in CCM and fixed switching frequency appears in Fig. 3. The principle consists of averaging the waveforms between the connecting terminals, "a" (active), "p" (passive) and "c" for common and of describing currents/voltages through a set of time-continuous equations. Vorpérian showed that configuring current and

voltage sources as in Fig. 3 was similar to considering an ideal dc transformer connected to terminals a-c-p and affected by a turns ratio d , the duty ratio.



Large-signal model for
dc and ac analyses.

Fig. 3. It is impossible to beat the PWM switch model in terms of simplicity!

The model is invariant meaning that it can be rotated to fit other dc-dc converters and all equations describing the PWM switch remain the same. The model presented in Fig. 3 is a large-signal version. Although SPICE can deliver a small-signal response from this model—because SPICE is a linear solver it will linearize the model prior to running the simulation—we cannot use it as is to determine a control-to-output transfer function. Instead, we need a linearized or small-signal version of the PWM switch. It appears in Fig. 4 where you see the general architecture and how it translates into a working SPICE model. For those interested in further details of the PWM switch, reference 2 thoroughly covers the topic with a lot of practical working examples.

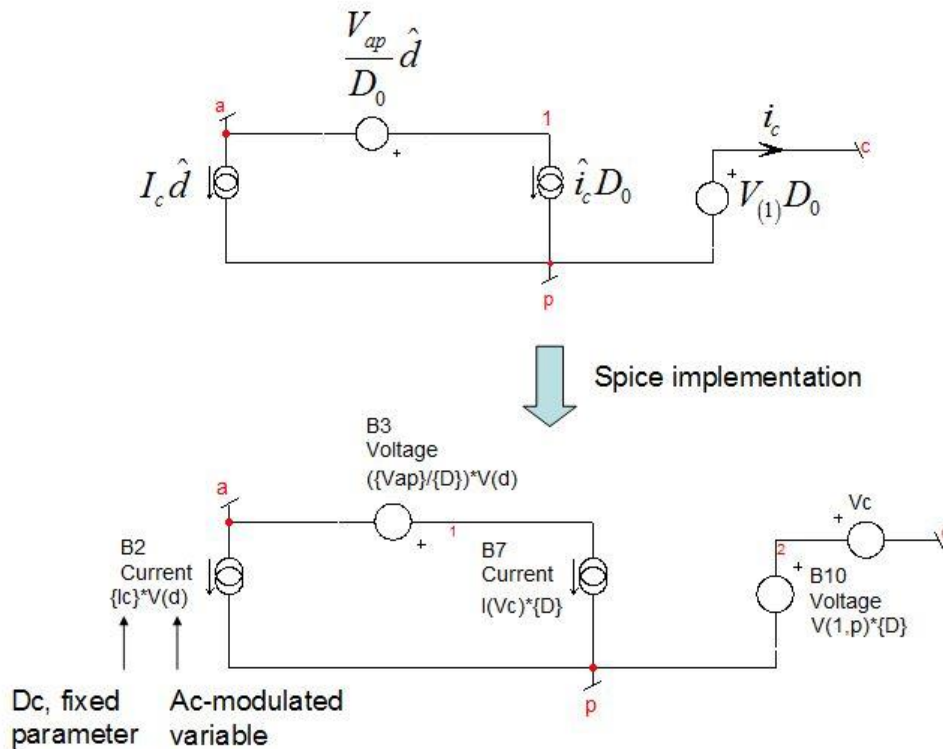
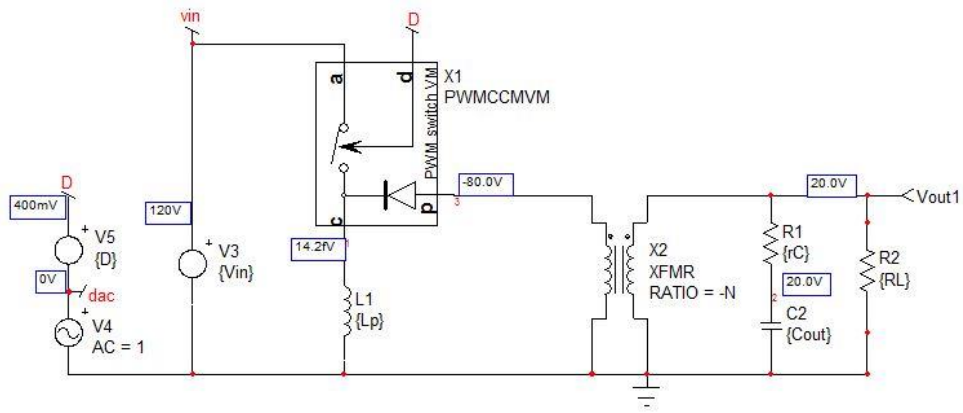


Fig. 4. The small-signal version of the PWM switch slightly complicates the original model.

Please note that sources made of several terms associate products of dc and ac values. For instance, the series source B3 shows a fraction made of $\{V_{ap}\}$ over $\{D\}$, multiplied by $V(d)$. $\{V_{ap}\}$ represents the steady-state voltage across terminals “a” and “p” while $\{D\}$ is the steady-state duty ratio. These are fixed parameters and correspond to one operating point. For instance, $\{V_{ap}\}$ in the buck converter of Fig. 3 is V_{in} . d , where the duty ratio can be any value between 0 V and 1 V (0 to 100%). $V(d)$ is the ac modulation (the \hat{d}) driving the model.

Fig. 5 shows how you simulate a flyback converter using the PWM switch model (top diagram) and its equivalent (bottom diagram) with the special transformer of ratio $1:d$. The two models are equivalent, electrically speaking but the transformer-based schematic truly shows the nature of the CCM PWM switch—an equivalent dc transformer controlled by the duty ratio—what the symbol does not immediately reveal. The framed voltages are the bias points calculated by the simulator. It is important to verify that they are within adequate limits. Sometimes the solver fails to determine the right operating point but a dynamic response is available. When that happens, it is obviously a wrong result and you must discard it until a new, correct operating point is found.



parameters

$N=0.25$
 $D=0.4$
 $Lp=600u$
 $RL=6$
 $Cout=100uF$
 $rC=1m$
 $Vin=120$
 $Vap=Vin+Vout/N$
 $Vout=N*D*Vin/(1-D)$
 $Ic=Vout^2/RL/(Vin*D)$

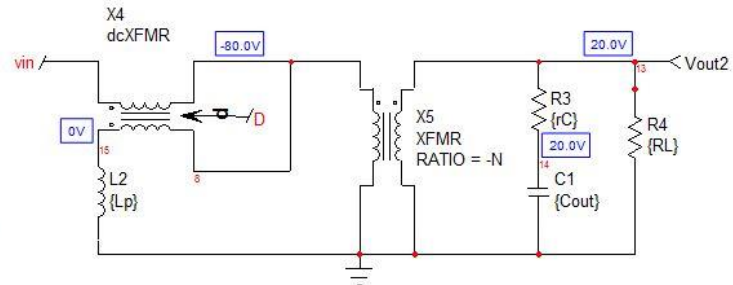


Fig. 5. A practical implementation of the large-signal PWM switch model in a CCM flyback converter.

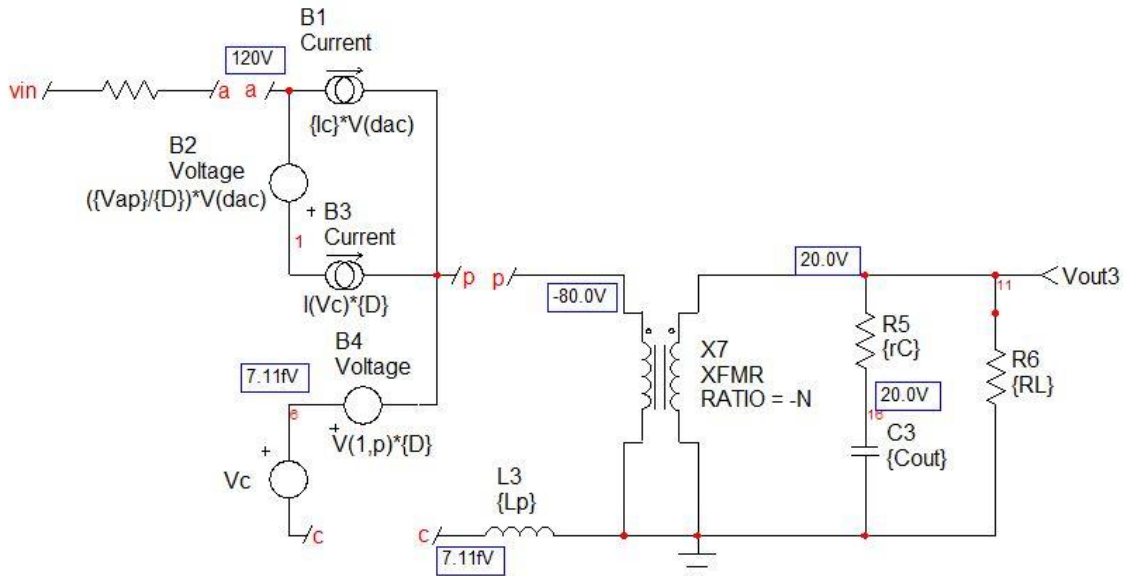


Fig. 6. The small-signal version of the PWM switch model in a CCM flyback converter requires a few controlled sources only.

From part 1, we know that the perfect (no leakage inductance) dc transfer function of the CCM flyback is

$$V_{out} = V_{in} \frac{ND}{1-D} = 120 \times \frac{0.25 \times 0.4}{1-0.4} = 20 \text{ V} . \quad (1)$$

This is what the schematic displays across the load resistance: our bias point is correct. Now that we have a large-signal model, we can unveil the small-signal implementation built on what has been presented in the bottom diagram in Fig. 4. The direct implementation of this model appears in Fig. 6. For this purpose, we need to calculate a few of the fixed parameters, V_{ap} and the average current in terminal "c", I_c . Once you have rotated the PWM switch model to fit the flyback converter structure, the voltage between terminals "a" and "p", V_{ap} , becomes equal to the input voltage V_{in} minus the reflected voltage, V_{out}/N (neglecting the secondary diode V_f). As this voltage is negative, we have

$$V_{ap} = V_{in} + \frac{V_{out}}{N} . \quad (2)$$

The current in terminal "c" is the average current flowing in the primary inductance L_p . Part of this current circulates in terminal "a" during the on-time or dT_{sw} and leaves through terminal "p" during the off-time or $(1-d)T_{sw}$. Fig. 7 shows the typical instantaneous waveforms for terminals "a" and "c". From the application schematic in Fig. 5, the average current in terminal "a" also circulates in the input source to create P_{in} :

$$P_{in} = I_a V_{in} . \quad (3)$$

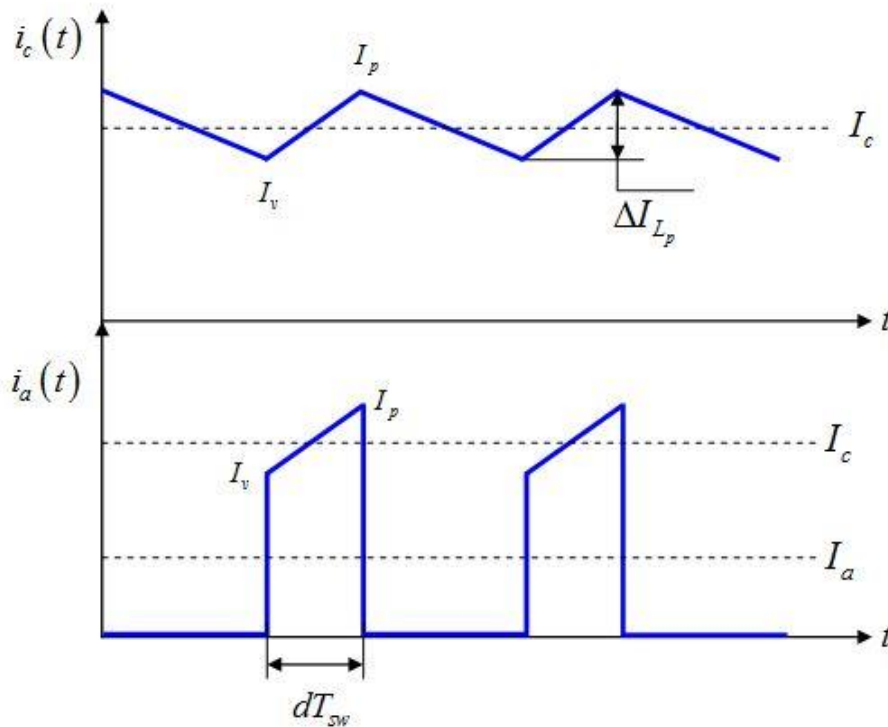


Fig. 7. The current in terminal "c" is that of the primary inductance L_p .

From Fig. 7, we can write

$$I_a = d \cdot I_c . \quad (4)$$

Substituting equation 4 into 3 and considering a 100% efficiency ($P_{in} = P_{out}$), we have

$$d \cdot I_c V_{in} = \frac{V_{out}^2}{R_L} . \quad (5)$$

Thus

$$I_c = \frac{V_{out}^2}{R_L \cdot d \cdot V_{in}} . \quad (6)$$

This expression is evaluated in Fig. 5's parameters window and passed as a parameter to the controlled sources (values between *brackets*{}). We can now run the simulation and gather all curves in a common graph. This is done in Fig. 8 and all curves (magnitude and phase) perfectly superimpose.

The results shown in Fig. 8 represent the classical response of a CCM flyback converter from the duty ratio input to the output. There is a peaking at the resonant frequency, then the ESR (equivalent series resistance, r_C) zero kicks in, followed by the RHP (right half-plane) zero, which brings the phase down further.

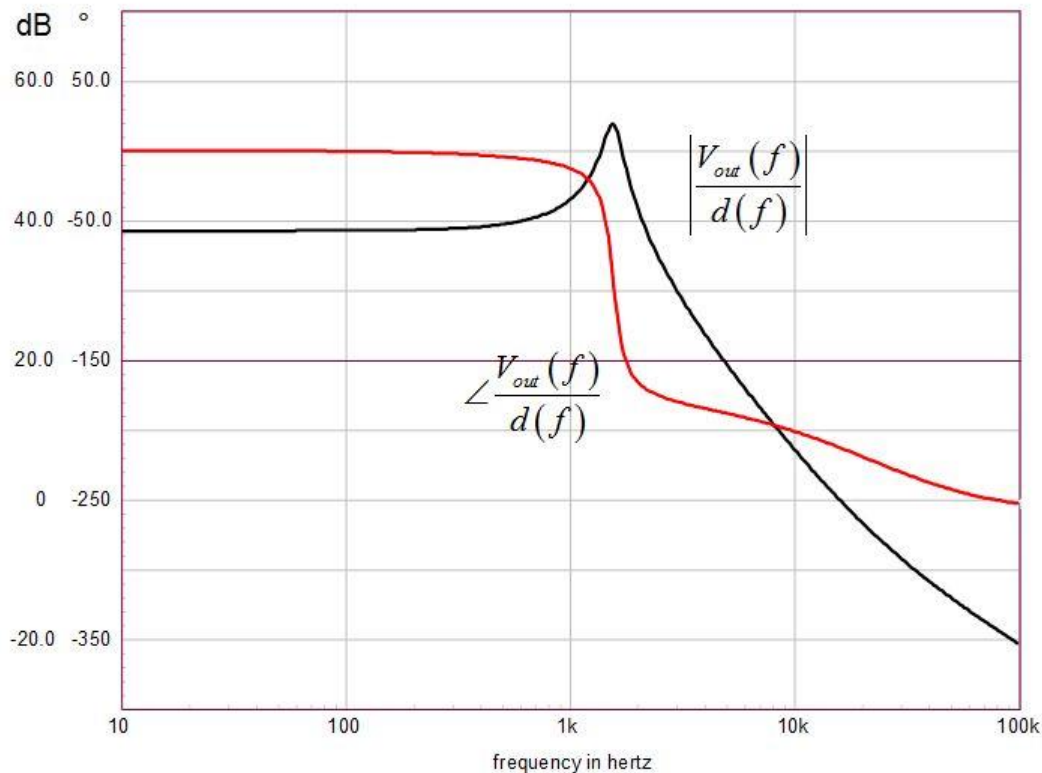


Fig. 8. Frequency responses obtained from the three different models (encapsulated large-signal model (Fig. 5 top circuit), transformer-based circuit (Fig. 5 bottom circuit) and the linearized version (Fig. 6 circuit) perfectly superimpose.

Considering The Leakage Inductance

In the average model presented in Fig. 5, the voltage applied to the model is V_{in} . This voltage biases the primary inductance L_p during dT_{sw} . In reality, as seen in part 1, considering the leakage inductance, the voltage splits between the leakage and primary inductances forming a voltage divider Div :

$$Div = \frac{L_p}{L_p + l_{leak}} \quad (7)$$

The first upgrade to the model is to replace V_{in} by $V_m \times Div$. The second change involves the duty ratio d . We have seen in part 1 that the duty ratio was affected by the leakage inductance magnetization time $d_1 T_{sw}$. The effective duty ratio applied to the average model needs to reflect this fact and is given by

$$d_{eff} = d - d_1 \quad (8)$$

where d_1 depends on the leakage inductance value by (neglecting the secondary-side diode drop V_f) and the valley current I_v .

$$d_1 = \frac{I_v l_{leak}}{\left(V_{in} + \frac{V_{out}}{N} \right) T_{sw}} \quad (9)$$

To calculate the valley current, we can look back at Fig. 7 and see that the valley current is actually the average current I_c minus half the primary inductance ripple:

$$I_v = I_c - \frac{\Delta I_{L_p}}{2} \quad (10)$$

The ripple current is the excursion brought by applying V_{in} over the series connection of L_p and l_{leak} during t_{on} or dT_{sw} . The valley current is thus

$$I_v = I_c - \frac{d_{eff} T_{sw} V_{in}}{2(L_p + l_{leak})} \quad (11)$$

The peak current is obtained in a similar way except that you reach it by adding half of the inductor ripple to I_c rather than subtracting it as in the above:

$$I_p = I_c + \frac{d_{eff} T_{sw} V_{in}}{2(L_p + l_{leak})} \quad (12)$$

The current circulating in the clamping network lasts $d_2 T_{sw}$, the leakage inductance reset time. This time depends on I_{leak} of course, but also on the reflected V_{out} and the clamp voltage V_{clp} . From part 1 we have determined the corresponding duty ratio to be

$$d_2 = \frac{I_p I_{leak}}{\left(V_{clp} - \frac{V_{out}}{N} \right) T_{sw}} . \quad (13)$$

Fig. 9 represents the various currents at play during the on-time. The bottom waveform is the power switch current and just above it, the current in the leakage inductance. When the switch turns off, we have seen that almost immediately (neglecting C_{lump} charging time), the current diverts into the clamping network and quickly goes down to zero (as seen in the top waveform.) At this moment, the leakage inductance is reset and the secondary current is at its peak.

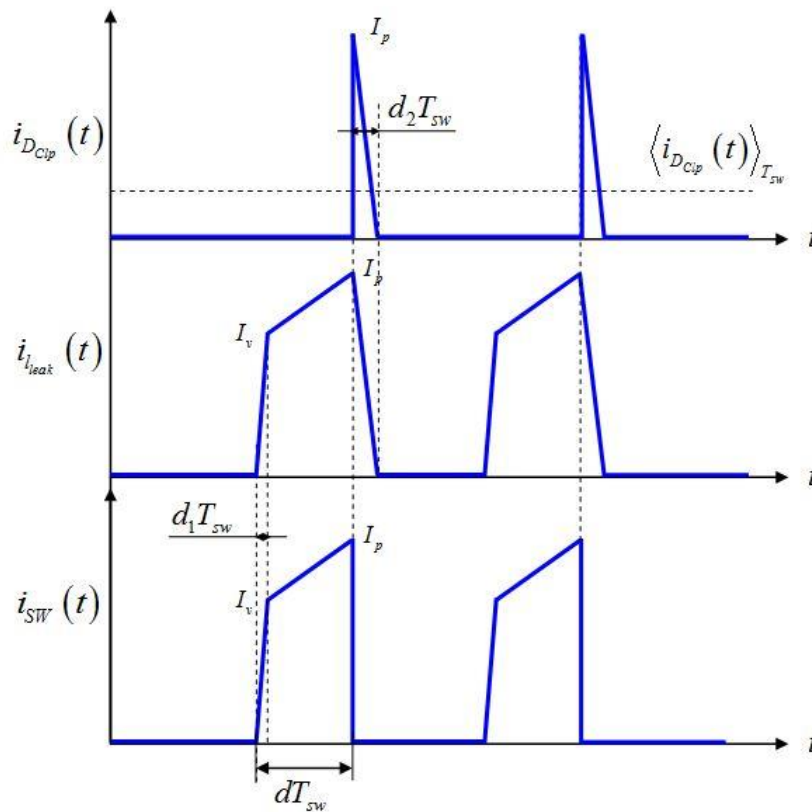


Fig. 9. The current circulates in the RCD network during the leakage inductance reset time $d_2 T_{sw}$.

The average current thus circulating in the clamp diode is simply the small triangle area averaged over the switching cycle:

$$\langle i_{D_{clp}}(t) \rangle_{T_{sw}} = \frac{1}{2} I_p d_2 . \quad (14)$$

Since I_p is computed by equation 12, we can connect an RC network across the current source modeled by equation 14 and we will obtain an averaged clamp voltage. In SPICE, this voltage will be used to determine d_2

as described by equation 13. The peak current in this equation depends on the output voltage applied across the load resistance. This voltage depends on d_1 as seen in part 1.

When you run the simulation, SPICE ends up solving a 6-unknown, 6-equation system and can sometimes fail to determine the right answer. To help it converge to the right result, a .NODESET statement telling it what "seed" to use will efficiently lead to the right bias point. That seed is the clamp voltage that we can suggest to SPICE prior to running it. The final large-signal model appears in Fig. 10. The added command line is .NODESET V(clp) = 300 V.

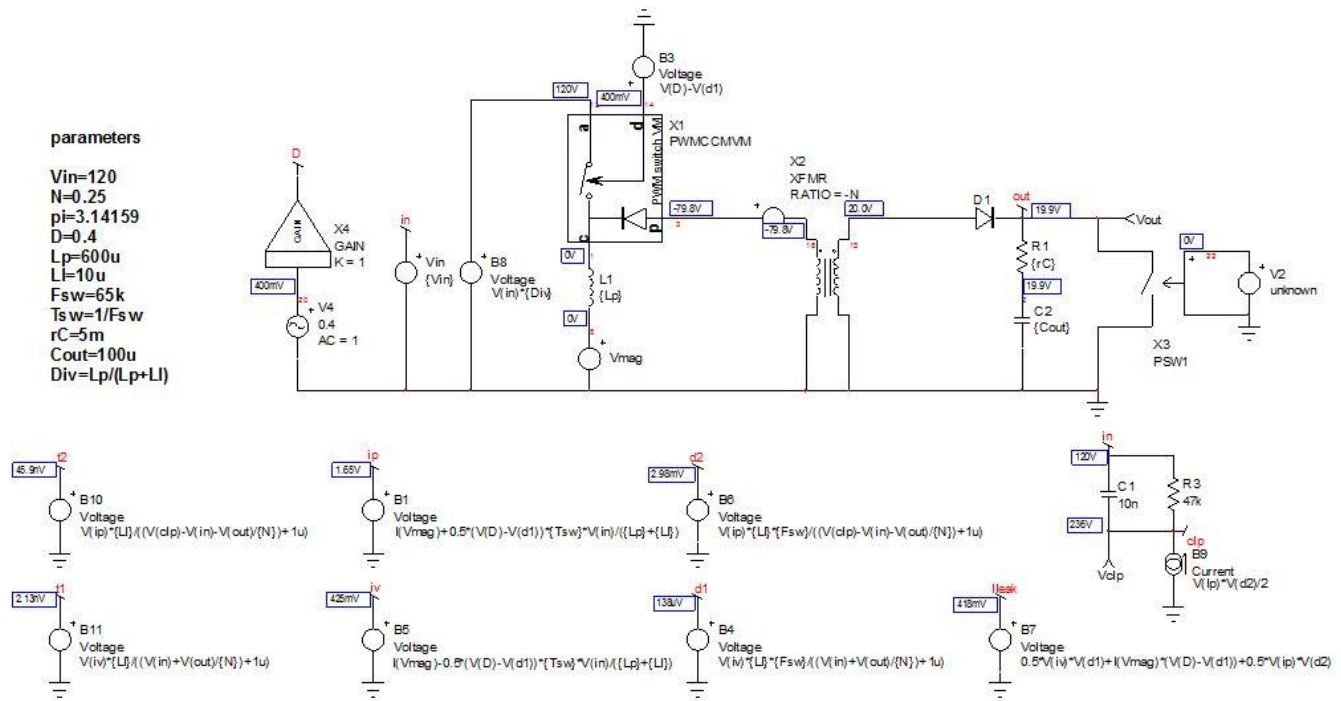


Fig. 10. The updated large-signal model now includes the leakage inductance contribution.

The exercise now consists of comparing the load-step response from the cycle-by-cycle model in Fig. 1 to that of the updated average model in Fig. 10. Several leakage inductance values are selected—1 μ H, 10 μ H and 30 μ H. As confirmed by Figs 11, 12, and 13, the agreement between the cycle-by-cycle model (red trace) and the average version (blue trace) is excellent.

The left-side of these figures shows the large-scale response while the right side shows a zoomed version confirming how well the averaged version tracks the cycle-by-cycle model (also known as the switched model.) A small discrepancy occurs in the clamp voltage, particularly in the dc level. This voltage depends on the t_2 duration, which can be of extremely small value. Any spread in the prediction of this parameter leads to a wide difference in the end.

Fig. 14 compares voltages observed at the clamp diode cathode in both models. Both curves match well despite the small difference in offset, which introduces a 2.5% error in this case. This error increases as I_{leak} does but keeps well within 10% for large I_{leak} values.

These experiments confirm that the large-signal model accounting for the leakage inductance matches the cycle-by-cycle version quite well and can consequently be considered for the linearization exercise.

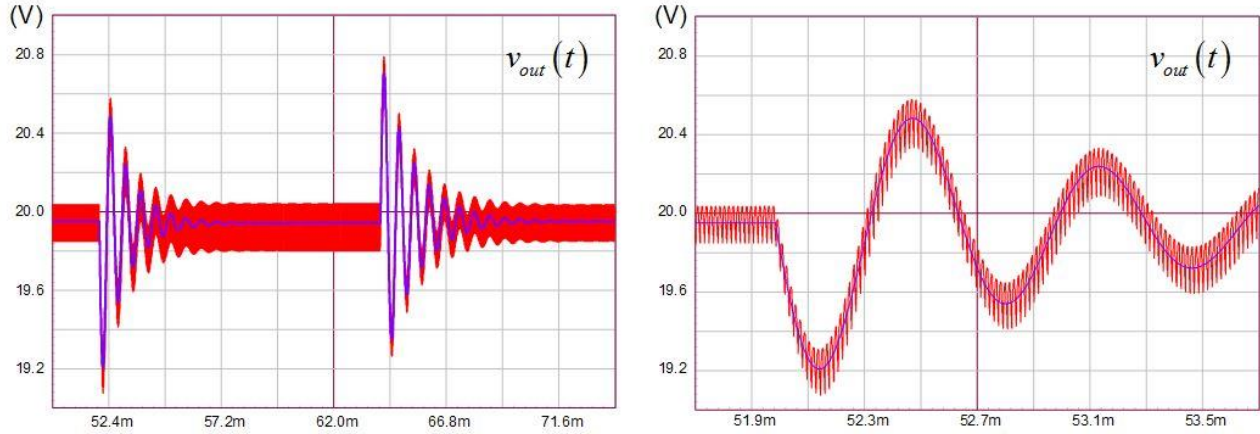


Fig. 11. Transient response for a 1- μH leakage inductance.

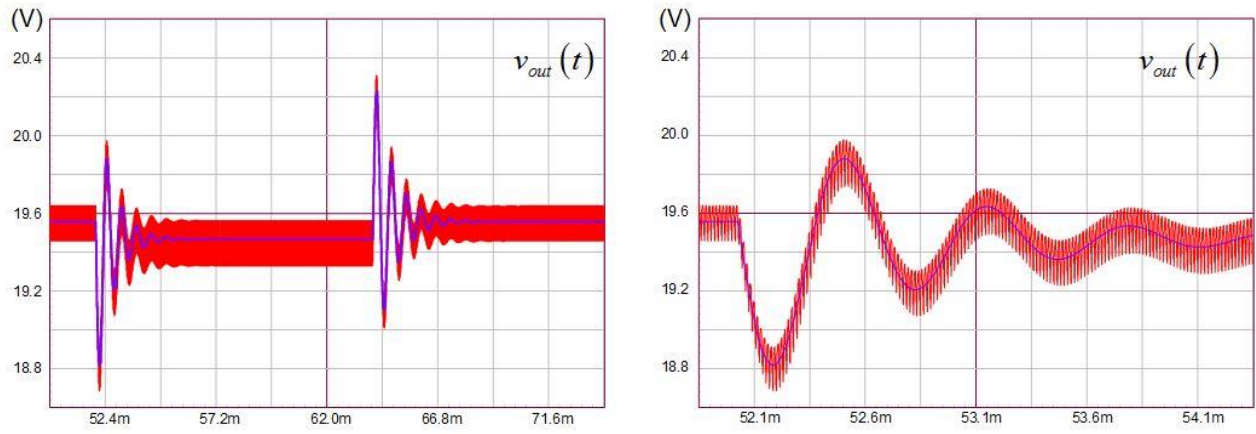


Fig. 12. Transient response for a 10- μH leakage inductance.

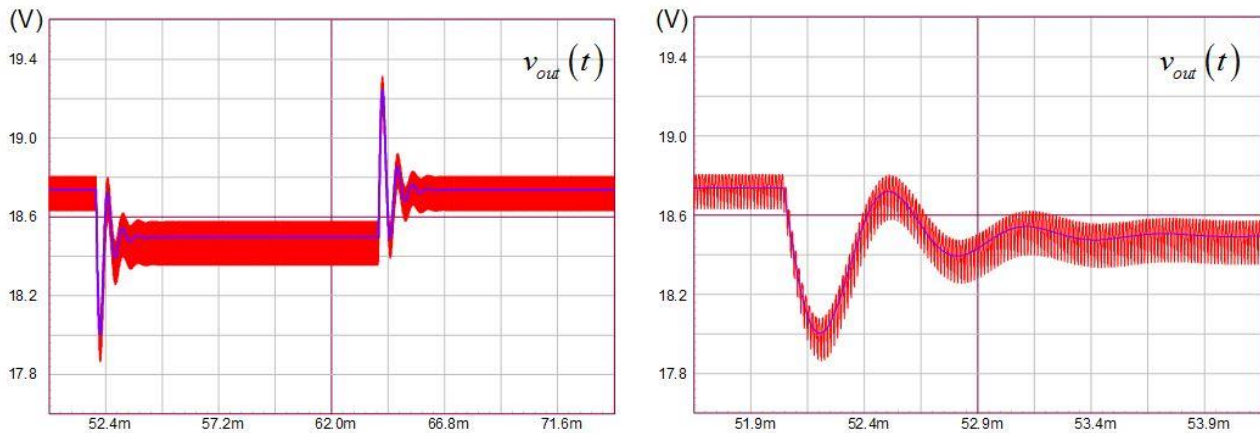


Fig. 13. Transient response for a 30- μH leakage inductance.

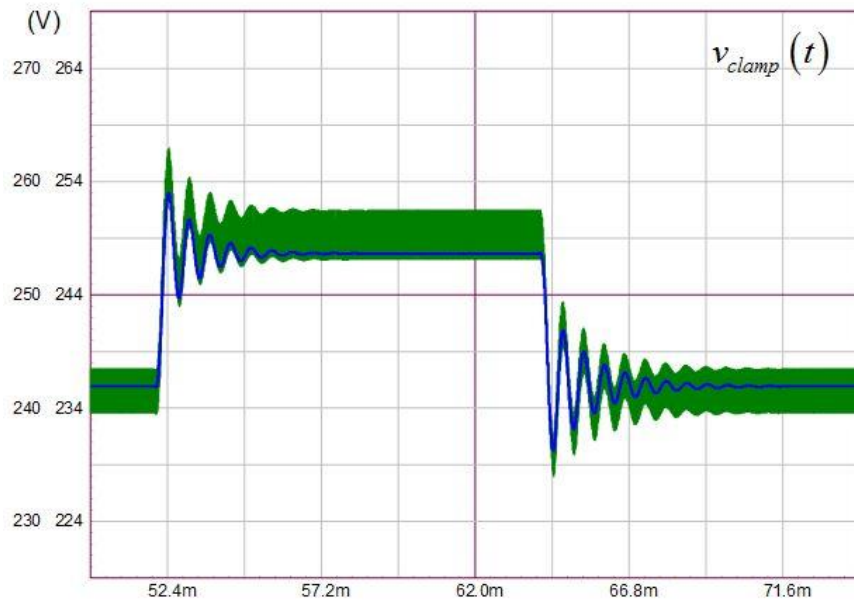


Fig. 14. The averaged clamp voltage (on the clamp diode cathode) tracks the cycle-by-cycle version fairly well ($I_{leak} = 1 \mu\text{H}$).

Conclusion

In this second part, we have seen how the leakage inductance damped the transient response of the flyback converter operated in CCM. Using the PWM switch model and including the leakage inductance contribution, we were able to build an average model mimicking the cycle-by-cycle version. This helped confirm that our approach was correct. It paves the way for the third and last part article in which we will derive the small-signal response of the converter.

References

1. "Simplified Analysis of PWM Converters Using the Model of the PWM Switch, Parts I (CCM) and II (DCM)," by V. Vorpérian, *Transactions on Aerospace and Electronics Systems*, vol. 26, no. 3, May 1990.
2. "Switch Mode Power Supplies: SPICE Simulations and Practical Designs," second edition by C. Basso, McGraw-Hill 2014, ISBN 978-0071823463.

About The Author



Christophe Basso is a technical fellow at ON Semiconductor in Toulouse, France. He has originated numerous integrated circuits among which the NCP120X series has set new standards for low standby power converters. SPICE simulation is also one of his favorite subjects and he has authored two books on the subject. Christophe's latest work is "Designing Control Loops for Linear and Switching Power Supplies: A Tutorial Guide."

Christophe received a BSEE-equivalent from the Montpellier University, France and an MSEE from the Institut National Polytechnique de Toulouse, France. He holds 18 patents on power conversion and often publishes papers in conferences and trade magazines.

For further reading on leakage inductance, see the How2Power [Design Guide](#) and enter "leakage inductance" in the keyword search. And for more on magnetics design in general, see the [Design Guide](#), locate the "Design Area" category, and click on the "Magnetics" link.